Coupling natural and electronic tags to explore spawning site fidelity and natal homing in northeast Atlantic European seabass

Emilie Le Luherne, Françoise Daverat, Mathieu Woillez, Christophe Pécheyran, Hélène de Pontual

Estuarine, Coastal and Shelf Science
November 2022, Volume 278, Pages 108118 (11p.)
https://doi.org/10.1016/j.ecss.2022.108118
https://archimer.ifremer.fr/doc/00799/91102/

Coupling natural and electronic tags to explore spawning site fidelity and natal homing in northeast Atlantic European seabass

Le Luherne Emilie [1], Daverat Françoise [2, *], Woillez Mathieu [1], Pecheyran Christophe [3], De Pontual Hélène [1]

[1] UMR DECOD (Ecosystem Dynamics and Sustainability), IFREMER, INRAE, Institut Agro, Brest, France
[2] INRAE, UMR ECOBIOP, Aquapôle INRAE, 64310, St Pée-sur-Nivelle, France
[3] CNRS/Université Pau & Pays Adour, Institut des Sciences Analytiques et de Physico-chimie pour l'Environnement et les Matériaux, UMR 5254, 64000, Pau, France

* Corresponding author : Françoise Daverat, email address : francoise.daverat@inrae.fr

Abstract :

The structure and connectivity of European seabass (Dicentrarchus labrax) populations remain poorly known and ecological evidence is missing to support the current delineation between the northern (southern North Sea, English Channel and Celtic Sea) and southern French stocks (Bay of Biscay). Adult spawning site fidelity and natal homing were analysed by coupling Data Storage Tag (DST) information and otolith microchemistry of recaptured fish to investigate, within the study area, the population structure and connectivity in European seabass. Trajectory reconstructions inferred from DST data were used to assign a spawning area (English Channel or Bay of Biscay) to each spawning winter record. In addition, otolith composition (Mg, P, Mn, Zn, Sr, Ba and δ18O) was measured in both larvae and adults otolith increments corresponding to a winter spawning event. We built a training dataset using coupled spawning area assignments and otolith elemental signatures (Mg, P, Mn, Zn, Sr and Ba) for winters with DST data. The training dataset was used to calibrate a Random Forest model and assign spawning areas based on otolith winter signatures outside the DST recording period. Results revealed that 64% of the seabass expressed spawning site fidelity. We also found a geographical gradient of site fidelity, with the highest proportions of spawning site fidelity found in seabass tagged at the northern and southern limits of the studied area. Significant ontogenetic effects were observed for trace elements and δ18O with ratios significantly lower in the larval stage than in the adult stage. These biases and the variability across cohorts prevented us to use the assignment model fitted on adults to study natal homing. At the larval stage, the analysis of spatio-temporal effects on otolith trace elements did not reveal any significant difference between spawning areas. However, the patterns of difference were similar for larval and adult Zn, Sr and Ba between the two spawning areas, suggesting a homing behaviour.

Graphical abstract

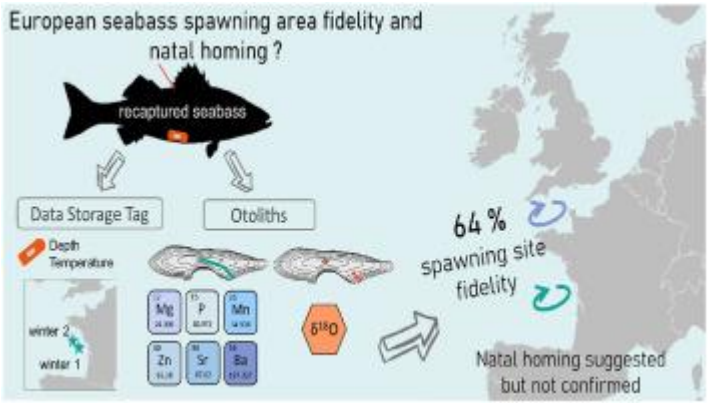

Highlights

► Investigation of seabass spawning site fidelity and natal homing. ► Data Storage Tag information was coupled to otolith microchemistry to infer spawning areas. ► Spawning site fidelity was found for 64% seabass individuals. ► Otolith tracers (elements and $\delta^{18}O$) were significantly biased by ontogenetic effects. ► Homing behaviour analysis provided inconclusive results.

Keywords : Spawning site fidelity, metapopulation, otolith microchemistry, Data Storage Tags, European seabass Dicentrarchus labrax

1. Introduction

The structure and connectivity of exploited fish species populations is a knowledge of major importance and the correspondence between stock management units and biological populations is a key issue for sustainable fishery management (Artetxe-Arrate et al., 2019). Yet, fisheries science has a long history of mismatches between stock management and the ecology of the target species, with potential threats to the sustainability of the resource (Kerr et al., 2017).

Population structure and connectivity are influenced by several environmental and biological factors throughout the life cycle of the fish (Kerr et al., 2017). At the adult stage, movements and survival are primarily driven by the essential habitat requirements of the fish. Among them, spawning site fidelity and natal homing are key processes affecting population differentiation and connectivity (Petitgas et al., 2013). Investigating the reproductive behaviour of fish is challenging and requires knowledge of the location of fish in the larval and adult stages to explore natal homing and spawning site fidelity processes. Under such constraints, the combination of direct and indirect estimates of fish location from electronic and natural tags appears to be a relevant and innovative choice (Fromentin et al., 2009). Data Storage Tags (DSTs) with pressure and temperature sensors are useful tools to explore fish movements as they provide data on individual fish behaviour over several years with high temporal accuracy (de Pontual et al., 2019). Individual trajectories are reconstructed based on the correlation between the

environmental parameters experienced by the fish and spatio-temporal reference fields derived from satellite observations and/or operational hydrodynamic models (Woillez et al., 2016). The record time of DSTs is now long enough to study spawning site fidelity, but this technology cannot provide useful data to explore natal homing. The analysis of otolith composition is the only alternative to study the movements of individuals throughout their entire life. Otoliths are calcified structures that incorporate environmental chemical signatures throughout the life of the fish. They have a great potential to provide indirect tracers of fish movements (Campana and Thorrold, 2001). Otolith elemental composition has been extensively used to discriminate fish stocks (Tanner et al., 2016). Among the elements used for these discriminations, Sr and Ba have been successfully linked to the mixing dynamics of fresh and marine waters and have proven to be robust spatial tracers for fish habitat occupancy across a wide range of ecosystems (Elsdon et al., 2008). The oxygen isotopic ratio ($\delta^{18}O$) of the otolith is also a relevant tool for fish geolocation as it differs between water masses with contrasting hydrology (LeGrande and Schmidt, 2006) and reflects temperature and salinity gradients (Trueman et al., 2012). Otolith $\delta^{18}O$ has been frequently used to identify the marine origin of fish and differentiate fish stocks (Darnaude and Hunter, 2017). Coupling electronic tag data with otolith composition appears well suited to study population structure and connectivity and has been successfully used to infer life traits such as growth, migration, and reproductive behaviour (Darnaude and Hunter, 2017).

European seabass (*Dicentrarchus labrax*) is a partially migratory species that inhabits the demersal waters of the northeast Atlantic. Its life cycle consists of an offshore phase in winter during which adults reproduce, followed by larval transport to coastal and estuarine areas, and a coastal phase in summer during which the juveniles establish for a few years and adults feed (Jennings and Pawson, 1992; Beraud et al., 2018). It is a key species for both recreational and commercial fisheries, assessed in the northeast Atlantic by the International Council for the Exploration of the Sea (ICES), which has defined four stocks (Fig. 1). The present study focussed on the two stocks separated by the 48th parallel north. The northern stock includes the English Channel, the Celtic Sea and the southern part of the North Sea. The southern stock corresponds to the Bay of Biscay, excluding the northern coast of Spain. The northern stock

98 declined to the point where the European Commission agreed on emergency conservation measures in
99 2015 (ICES, 2020a, 2020b). A better understanding of the spatio-temporal population structure and
100 dynamics is needed to improve management, as evidence is missing to support the current delineation
101 of these stocks (de Pontual et al., 2019). Genetic analyses revealed two lineages, one Mediterranean
102 and one Atlantic, with a weak genetic structure for the Atlantic population (Souche et al., 2015).
103 However, using the percentage of Mediterranean introgressive hybridisation in the genome of Atlantic
104 seabass populations, Robinet et al. (2020) showed that the tip of Galicia and the Cotentin peninsula act
105 as barriers to gene flow. The authors also suggested a subtle structure of the Bay of Biscay and the
106 western English Channel populations compared to those of the eastern English Channel. Further
107 evidence of a spatio-temporal population structure was provided by DST data in Western Brittany (i.e.,
108 around the 48th parallel north (de Pontual et al., 2019). Western Brittany was found to be a feeding area
109 where populations mix in summer when adult fish migrate between winter spawning areas and summer
110 feeding grounds, showing fidelity to both essential habitats (de Pontual et al., 2019). Few western
111 Brittany seabass have resident behaviour (de Pontual et al., 2019), suggesting that they have alternative
112 spawning strategies.

113 The aim of the present study was to analyse the spawning site fidelity and natal homing of the northeast
114 Atlantic seabass population. This was performed by coupling fish location inferred from DST data and
115 otolith microchemistry from recaptured fish. The hypothesis was that otolith composition matching with
116 DST derived locations during spawning events was different between English Channel and Bay of Biscay.
117 We assumed that coupled DST location-otolith composition during spawning events was a reference
118 (set up into a model of assignation), that could be used to retrieve fish spawning area inferred from
119 otolith composition outside the DST period. Otolith trace elements were therefore used as proxies of
120 fish location. Natal homing was explored using otolith microchemistry at the larval and adult stages on
121 individuals that had expressed spawning site fidelity.

122

2. Material and methods

2.1. Sample collection

The samples were taken from wild seabass recaptured after tagging during a large-scale DST tagging program carried out by Ifremer in the English Channel (EC) and the Bay of Biscay (BoB) in 2014-2016 (Fig. 1). Recaptured seabass came from either the commercial or the recreational fisheries. Among the 470 (38.5%) tags recovered by August 2021 out of the 1220 tagged seabass (de Pontual et al., submitted), 42 recaptured fish were selected based on a minimum of two winters of freedom after tagging (Supp. Mat. 2). Scales were collected on each individual seabass at tagging and recapture, with otoliths collected at recapture. Analyses were conducted in the first quarter of each year (winter) as the seabass spawning season extends from January to March in the Bay of Biscay and from February to April in the English Channel (e.g., Dambrine et al., 2021). Spawning areas were designated as the English Channel (EC) for the northern seabass stock and the Bay of Biscay (BoB) for the southern seabass stock.

2.2. Calcified structures selection and analysis

Right otoliths were used for $\delta^{18}O$ analysis and, left otoliths were used for trace element analysis. Otoliths were embedded in epoxy resin for both analyses. The transverse sections were ground with ultra-pure water and silicium carbide paper to reach the nucleus and ensure high flatness of the otolith sections.

2.2.1. Age estimation

No standard protocol for seabass age estimation based on otolith increment counting was available, and an indirect validation of seabass age was obtained by comparing scales collected during tagging and otolith and scales collected at recapture. Age was estimated by three readers. Each circulus for scale and annulus for otolith was counted as one year (Supp. Mat. 3). Finally, the otolith chronology was obtained by identifying otolith annuli corresponding to the winter periods recorded by the DST.

2.2.2. Trace element ratio – LA ICP-MS analysis

147 The elemental analyses were performed using a high-resolution inductively coupled plasma mass
148 spectrometer (ICP-MS), Thermo Element XR, coupled to a high repetition rate UV femtosecond laser
149 ablation system, Lambda 3 (Amplitude system, France), at the IPREM PAMAL platform in Pau (France).
150 Calibration, sampling design and instrumental bias correction of LA ICP-MS analysis are available in
151 Supp. Mat. 4. Otolith material was ablated on transects from the nucleus to the dorsal edge,
152 perpendicular to the growth increments. Transects consisted of a 20 µm wide central line, a scanner
153 speed of 1 mm.s^{-1} and a deck speed of 5 µm. s^{-1}. The following elements were quantified: ^{25}Mg, ^{31}P, ^{43}Ca,
154 ^{55}Mn, ^{66}Zn, ^{88}Sr and ^{138}Ba. The average detection limits (µg·g^{-1}) LOD achieved in this study were as
155 follows: ^{25}Mg 0.51, ^{31}P 3.49, ^{43}Ca 250, ^{55}Mn 0.12, ^{66}Zn 1.07, ^{88}Sr 0.39, ^{138}Ba 0.14. The P concentrations
156 along the otolith transects showed seasonal patterns (Heimbrand et al., 2020) synchronised with the
157 otolith structure, allowing the delimitation of winter sequences. The larval stage was delineated using
158 otolith structure and maximum P concentration within the nucleus region (Thomas and Swearer, 2019).
159 For each larval stage and each winter sequence, the mean of the seven elements was calculated.

160 2.2.3. Oxygen isotope ratio – SIMS analysis

161 The $\delta^{18}O$ analyses of the otolith were performed on a CAMECA IMS 1270 ion microprobe at the
162 Edinburgh Ion Microprobe Facility (UK). Triplicate $\delta^{18}O$ point measurements were performed in the
163 nucleus area (larval phase) and in the DST recorded winter bands. A transect of 61 points from the core
164 to the edge was also performed to validate the position of winters according to $\delta^{18}O$ values. We provide
165 the calibration, the sampling design and the instrumental bias correction of the SIMS analysis in Supp.
166 Mat. 5. All the $\delta^{18}O$ values were reported in per mil ‰ relative to SMOW. We used the following
167 equation to convert $\delta^{18}O$ values from SMOW to PDB (Coplen et al., 1983):

168 $$\delta^{18}O_{PDB} = 0.97002\ \delta^{18}O_{SMOW} - 29.98 \quad \text{(eq. 1)}$$

169 When several measure points were available per life stage, the mean of the $\delta^{18}O$ values was used.

170 2.2.4. Oxygen isotope ratio – Prediction of otolith $\delta^{18}O$

Predicted otolith $\delta^{18}O$ values were estimated at the EC and BoB spawning areas (Fig. 1) during the spawning events from 2003 to 2018 for larval and adult stages. Estimates were based on daily temperature and salinity predicted by the Atlantic Margin Model FOAM with a 49 km² resolution grid (UK Met Office Operational Suite, https://marine.copernicus.eu/) for northern Cotentin (-1.95 to -1.64 °W and 49.97 to 50.21 °N) and the Rochebonne Plateau (-2.60 to -2.29 °W and 46.04 to 46.28 °N), within the main spawning hotspots of the EC and BoB stocks (Dambrine et al., 2021; Fig. 1), respectively. Daily winter (from January to March) temperature and salinity from the surface to 30 m deep were extracted to study the larval stage (Jennings and Pawson, 1992) and those from the surface to 150 m to study the adult stage (Woillez et al., 2016).

Oxygen isotope ratios of ambient seawater ($\delta^{18}O_{sw}$) were estimated from salinity (S) using the following equation applied to the North Sea (Harwood et al., 2008):

$$\delta^{18}O_{sw\ SMOW} = 0.274 \times S - 9.3 \quad \text{(eq. 2)}$$

$\delta^{18}O_{sw\ SMOW}$ were then converted into $\delta^{18}O_{sw\ PDB}$ using equation eq. 1. Finally, we used the theoretical equation for inorganic aragonite deposition to predict $\delta^{18}O_{otolith\ PDB}$ (Kim et al., 2007):

$$1000\ ln\alpha = \left(17.88 \times \frac{1000}{T}\right) - 31.14 \quad \text{(eq. 3)}$$

with $\alpha = \frac{1000 + \delta^{18}O_{otolith}}{1000 + \delta^{18}O_{sw}}$ and T, the temperature in Kelvin.

2.3. Reproductive event validation and spawning area attribution

Data were treated as specified in Fig. 2. Spawning events were defined as winter months in the otolith calendar following age at maturity (> 5 yo for males and > 6 yo for females; Pickett and Pawson, 1994). DST data were used as validation as follows: spawning events covered by DST records were identified when depth was greater than 30 m during the first quarter of the year (Pickett and Pawson, 1994; Pawson et al., 2007; Supp. Mat. 2). Spawning area (i.e. EC or BOB stock areas) was assigned to an otolith spawning event, based on the corresponding DST derived position using the average location of the

individual reconstructed trajectory computed over the spawning month showing the highest vertical movements (Woillez et al., 2016; de Pontual et al., submitted). Skip spawning outside the period recorded by DST, could not be considered as otoliths and scales of seabass do not record past spawning events. We used the hypothesis that seabass reproduced each year after the DST recorded period provided it matched with age at maturity.

2.4. Data analysis

2.4.1. Comparison of predicted and measured otolith $\delta^{18}O$

An ANOVA was performed to test the effects of life stage, year and spawning area on predicted otolith $\delta^{18}O$ values. Another ANOVA was used to test the effect of life stage on otolith $\delta^{18}O$ measurements.

2.4.2. Adults' fidelity to spawning areas

Normal distribution was not reached for any of the tracers, hence, a non-parametric PERMANOVA was used to test if the microchemical elements varied spatially and annually (Anderson, 2017). This investigation was first performed on the training dataset, i.e., the coupled DST-otolith elemental signatures. We then used the Random Forest (RF) algorithm to explore seabass spawning site fidelity (Mercier et al., 2011). The calibration of the RF model (number of trees = 500, mtry = 2) was performed on coupled DST-otolith elemental signatures (Mg, P, Mn, Zn, Sr and Ba) (Fig. 2). To deal with the imbalanced training dataset, cut-off parameter was tuned by the proportion of the rare class (EC spawning area). The assignment of a spawning area by the RF model was limited to a maximum of two years before and after DST records. The calibrated RF model was used to predict spawning areas for winters outside the DST recording period (Fig. 2). Spawning site fidelity was identified when the sequences of the spawning area assigned to each year by the RF model had similar spawning areas for all consecutive winters. The contribution of the tracers to the discrimination of EC and BoB spawning areas was studied with a PCA applied to individuals expressing spawning site fidelity.

220 2.4.3. Natal homing

221 The effect of life stages on elemental composition was tested with a PERMANOVA. We hypothesised
222 that these fish were born in the same area where they had spawned repeatedly (Fig. 2) by comparing
223 otolith larval signatures between adult spawning origins (either EC or BoB).

224

225 ## 3. Results

226 Of the 42 seabass in this study, 25 were tagged along the BoB coast and 17 along the EC coast (Supp.
227 Mat. 2). The age of the seabass ranged between 6 and 18 years old at the time of recapture (Supp. Mat.
228 2). There were 27 females, 13 males and 2 undetermined sex (Supp. Mat. 2). The study encompassed
229 143 effective spawning events, including 74 coupled DST-otolith elemental signatures. Effective
230 spawning events were recorded between 2003 and 2018 with a majority of events between 2014 and
231 2017, and mainly for seabass between 6 and 8 years old (Supp. Mat. 2). Larval signatures were available
232 from 1998 to 2011, with a majority of larval signatures between 2007 and 2009 (Supp. Mat. 2).
233 The reconstructed trajectories inferred from the DST data assigned 19 spawning events to the EC and
234 55 offshore spawning events to the BoB (Supp. Mat. 6). Two individuals (DK_A10572 and DK_A10591)
235 tagged and recaptured in the EC had been allocated to the BoB spawning area using trajectory
236 reconstruction, but this was found to be highly unlikely (de Pontual et al., submitted). We thus
237 performed the analysis by assigning them first to the EC spawning area (Supp. Mat. 6) and then to BoB
238 spawning area (Supp. Mat. 7 Table 7.2).

239

240 3.1. Oxygen isotope ratios

241 The predicted $\delta^{18}O$ values were very close in both larvae and adult (Supp. Mat. 8.a). The ANOVA revealed
242 significant differences between years and spawning areas for larval (year: $F_{1,2881}$ = 38.38; p = <0.001;
243 spawning site: $F_{1,2881}$ = 3907.34; p = <0.001) and adult stages (year: $F_{1,2881}$ = 38.70; p = <0.001; spawning

site: $F_{1,2881}$ = 3873.85; p = <0.001) (Supp. Mat. 8.a). The predicted $\delta^{18}O$ were consistently higher in the EC than in the BoB over time, with a mean difference of 0.4 PDB. The difference varied between years, with overlapping values between areas in 2006 and 2007. The minimum difference was observed in 2005 and the maximum difference in 2011 (Supp. Mat. 8.a).

The ANOVA revealed a significant difference between stages, with the adult signatures being higher ($F_{1,112}$ = 290.13; p = <0.001 ; Supp. Mat. 8.b). This $\delta^{18}O$ difference between stages was also evident on otolith transects between the nucleus to the edge throughout the life of the seabass (Supp. Mat. 9). Along this $\delta^{18}O$ "life transect", $\delta^{18}O$ variations were found to show seasonal patterns that matched the structure of the otoliths (Supp. Mat. 9). The difference in measured $\delta^{18}O$ was not obvious between spawning areas, and the $\delta^{18}O$ differences observed between spawning areas for adult otoliths varied between years (Supp. Mat. 8.b).

The inter-annual variation in $\delta^{18}O$ measured at the adult stage between spawning areas and the significant effect of the stage precluded the use of $\delta^{18}O$ as a location tracer in this study. Therefore, the study of spawning site fidelity and natal homing was based on elemental signatures only.

3.2. Spawning site fidelity

Within the training dataset, adult otolith signatures were significantly different between the EC and the BoB spawning areas for Zn, Sr and Ba (Fig. 3). Although P, Zn and Sr varied significantly between years, the effect of spawning area on Zn and Sr overweighed this temporal effect (Fig. 3 and Table 1). We detected a significant interaction between spatial and temporal factors for Zn (Table 1). Sr increased in the BoB between 2015 and 2018 (Fig. 3). Zn and P decreased between 2015 and 2018 in both spawning areas with consistently higher Zn concentrations in the EC than in the BoB (Fig. 3). A RF model was fitted using the 74 otolith trace element signatures of the training data set (Fig. 3 and Supp. Mat. 5 and 6). The RF model was then used to assign spawning areas to the 69 spawning events of unknown location. The resulting RF model had an average OOB error rate of 25.68 %. The assignment error was consistent

for both spawning areas (EC: 21 % and BoB: 27 %). The Gini index indicated that Ba, Zn and Sr (6.72, 6.7 and 4.9, respectively) were the main elements used for the classification followed by Mn, P and Mg (3.9, 2.9 and 2.7, respectively). We assessed the sensitivity of the expert-corrected RF model by comparing its spawning area assignment results for DK_A10572 and DK_A10591 with DST data (expert and DST) (Supp. Mat. 7). Assigned spawning areas remained virtually unchanged, except for the two individuals tagged at DK and one tagged at LT (Supp. Mat. 7).

Individuals with only a single winter of otolith signature were excluded from the analysis (CB_A11114, LT_A11243 and IO_A12484; Supp. Mat. 2). The analysis of seabass spawning site fidelity was based on 140 spawning events (71 DST and 69 RF spawning area assignments), and a total of 36 seabass over a period of 2 to 6 years (Supp. Mat. 6). Our results revealed that 64 % of the seabass expressed spawning site fidelity (23 seabass; Supp. Mat. 6).

Our results showed geographical patterns in site fidelity, with spawning site fidelity most often expressed by seabass tagged at locations near either the northern limit of the EC stock or the southern limit of the BoB stock (Fig. 1 and Supp. Mat. 6). Most of the seabass tagged in the western part of the EC (with the corresponding tagging sites SM, SQ and SV, Fig. 1) have moved between the EC and the BoB (Supp. Mat. 6). Hence, the group of seabass tagged in the western part of the EC had the highest proportion of individuals alternating spawning migrations between the EC and the BoB over the years. None of the seabass with a predicted spawning area in the previous two years and tagged at NO site expressed fidelity to their spawning site (Supp. Mat. 6). The RF model assignment of NO site spawning signatures to the EC can be attributed to the lower values of Sr and Ba used in the prediction dataset compared to the training dataset (Supp. Mat. 10 and 11). Spawning site fidelity was more frequently found for the 27 female seabass (70% fidelity) compared to the 13 male seabass (46 % fidelity).

The results of the RF model were mainly driven by the high Sr and Ba concentrations, as shown in the first axis (37 % of the variance) of the PCA plot (Fig. 4). The contribution of Zn and Mn was lower. Most of the BoB signatures had higher Sr and Ba concentrations than the EC signatures (Fig. 4). The second

294 axis of the PCA explained 26 % of the variance and divided the data according to high Zn and high Mn
295 concentrations (Fig. 4). Most of the EC signatures lied along this second axis, from high Zn
296 concentrations to high Mn concentrations.

297 3.3. Natal homing

298 For the 23 seabass that had expressed fidelity to a spawning area, difference between larval and adult
299 element signatures was significant for all the tracers (PERMANOVA, R^2 = 0. 576; $F_{1,224}$ = 293.66; p =
300 0.001) and the bias was not constant over individuals. This precluded the use of the RF model adjusted
301 on adult signatures to assign birth locations based on larval signatures.
302 No significant difference in trace element concentrations of the larval otolith between the two spawning
303 areas (PERMANOVA, R^2 = 0. 074; $F_{1,21}$ = 1.697; p = 0.227). However, the differences in spawning areas
304 between larval signatures for Zn, Sr and Ba followed the same patterns of differences as for the adult
305 stage (Fig. 5). Although the difference was not significant, the plot of log-transformed otolith trace
306 elements for the larval and adult stages suggested that both Sr and Ba were lower in the EC than in the
307 BoB (Fig. 5). This pattern suggests that the seabass spent their larval stages in the same area where they
308 returned to spawn as adult fish.

309

310 ## 4. Discussion

311 To the best of our knowledge, the present work is one of the few studies coupling DST reconstructed
312 trajectories with otolith structure or chemistry (Hüssy et al., 2009; Bardarson et al., 2017; Darnaude et
313 al., 2014; Jónsson et al., 2021). Only Darnaude et al., (2014) used a similar method to infer *a posteriori*
314 adult fish geolocation, using only one otolith tracer. The number of samples (42) was small but provided
315 important insights into seabass spatial segregation and spawning site fidelity. Our approach provides a
316 unique insight into the life histories of individual seabass, supporting spawning site fidelity and
317 suggesting natal homing.

4.1. Evidence of spawning site fidelity in a temperate marine fish

Assessing the structure and connectivity of fish populations is essential for achieving sustainable fisheries management (Artetxe-Arrate et al., 2019). Studying spawning site fidelity, one of the key processes affecting the structure of fish populations, is therefore fundamental (Petitgas et al., 2013). Our results revealed that 64 % of the seabass express spawning site fidelity either to the English Channel or the Bay of Biscay spawning areas. These results tend to confirm the delineation of the population revealed by tag-recapture (Fritsch et al., 2007) and trajectory reconstruction studies (de Pontual et al., 2019). A delineation of the seabass population was not found in previous genetic studies due to the high level of gene flow (Fritsch et al., 2007; Souche et al., 2015).

The results are relevant because of the low uncertainties in the reconstruction of the DST trajectories and the discrimination of spawning areas from otolith microchemistry data. The spatial resolution (several hundred kilometres) was relevant for correctly assigning locations based on temperature and depth (trajectories from DSTs) and locations based on elemental ratios. Current geolocation models have average errors of about 30–50 and 120 km for demersal and large pelagic fish, respectively, which is acceptable for studies at the scale of fisheries management units (Gatti et al., 2021). We used trajectory reconstructions based on an improved version of a published geolocation model developed for seabass in the Iroise Sea (Woillez et al., 2016). This version was improved to address a larger geographical scale and a wider range of migration strategies as well as newly encountered behaviours (de Pontual et al., submitted). The sensitivity analyses and simulation-estimation experiments demonstrated that the original geolocation model was reliable (Woillez et al., 2016). Here, two individual trajectories of seabass tagged at DK were considered uncertain as they differ from the migration strategy of most individuals tagged at the same site (de Pontual et al., submitted). Following the expert opinion, the DST data recorded for these specific individuals and years were assigned to the EC. However, the alternative spawning area given by the model did not change significantly the overall results of the RF model (Supp. Mat. 7).

We delineated spawning periods base on otolith structure and high P concentrations that clearly identify winters (Hüssy et al., 2020; Heimbrand et al., 2020). This temporal proxy of adult spawning events corresponds to seabass spawning periods of three to four months in the EC and BoB (Dambrine et al., 2021). Seabass remain in the winter spawning areas for at least one month before moving to their summer feeding areas (Fritsch et al., 2007). However, seabass have the ability to move rapidly across large distances and display large vertical movements (de Pontual et al., 2019). The resulting otolith signatures of fast moving fish would be difficult to interpret, due to the incorporation dynamics of elements into the otolith making it difficult to identify an accurate reference signature of the spawning events. Another uncertainty came from the impossibility to consider skip spawning outside the DST recorded period, despite the fact it might be as common for seabass as for other species (Rideout and Tomkiewicz, 2011). As skip spawning was only observed in 4 seabass and not for two consecutive years (Supp. Mat. 2), skip spawning did not seem very frequent.

The potential of otolith microchemical tracers to discriminate marine water masses has been demonstrated previously (e.g., Thorrold et al., 2001; Darnaude et al., 2014). The Sr, Ba and Zn signatures of adult otoliths were found to discriminate the EC from the BoB. Our results revealed higher Sr and Ba concentrations in the BoB than in the EC. Although the Sr difference between the spawning areas may be attributed to the positive correlation between Sr and salinity (Elsdon et al., 2008), as salinity is higher in the Atlantic and the Bay of Biscay than in the English Channel (Ayata et al., 2010), the salinity difference is small between the BoB and the EC and overall Sr in seawater is quite uniform (de Villiers, 1999). The difference in seabass otolith Sr would rather be an indirect indication of a difference of temperature between BoB and EC, and driven by a difference of growth. The Ba difference could be mainly due to the high concentration of Ba in seabass tagged at CB, NO and IO, possibly correlated with time spent either in the estuarine plume (Elsdon and Gillanders, 2005) or in deep water (Wolgemuth and Broecker, 1970), which corresponds to the location of IO near the mouth of the Gironde Estuary and CB near the submarine canyon in the gouf of Capbreton. Sr and Ba are known to be robust tracers for juvenile seabass trajectories (Reis-Santos et al., 2013) and have been shown to discriminate marine

areas (Soeth et al., 2019). While predicted $\delta^{18}O$ significantly discriminated the EC and the BoB, oxygen isotopes measured in seabass otoliths failed to discriminate the BoB from the EC spawning areas. In other marine contexts, the $\delta^{18}O$ measured in otoliths was successfully linked to the $\delta^{18}O$ of ambient water (Artetxe-Arrate et al., 2021), making it an efficient and predictable tracer of seawater mass occupancy (von Leesen et al., 2021). Moreover, using entire dissolved otoliths, Neves et al. (2019) found a significant difference for black seabreams between the EC and the BoB with higher $\delta^{18}O$ in the EC than in the BoB. The IRMS method used by Neves et al. (2019) is more accurate than SIMS but requires a larger amount of sample, which is incompatible with the amount of otolith material that can be collected during a spawning event (Pinto et al., 2021).

Our study also revealed a geographical feature in spawning site fidelity with seabass tagged at the northern (DK) or the southern (CB) limits of the study area expressing more frequent spawning site fidelity than seabass tagged in Brittany near the limit of the two stocks studied (e.g., SQ and AD). These results are consistent with those of de Pontual et al. (2019). Iroise Sea appears as a major biogeographical frontier between temperate and cold temperate marine assemblages (Ayata et al., 2010). Movements outside spawning areas appear to be fairly common for this species (Pickett et al., 2004; Fritsch et al., 2007; de Pontual et al., 2019). This behaviour has been associated with the use of alternative summer feeding habitats along Brittany coast (de Pontual et al., 2019). Indeed, reconstructions of the trajectories of seabass tagged in Western Brittany have revealed individuals spawning either in the EC or in the BoB, as well as individuals residing permanently in the Iroise Sea (de Pontual et al., 2019). Despite the imbalanced sex ratio of the sample, spawning site fidelity of female seabass was greater than the spawning site fidelity of male seabass. A female-biased homing behaviour was already observed for swordfish (Muths et al., 2009) and bluefish (Miralles et al., 2014). Male-biased site fidelity was found in a species expressing a strong territoriality (Cresci et al., 2022). For species with a female-biased sexual size dimorphism such as observed for seabass (Saillant et al., 2001), the male-male competition is decreased (Horne et al., 2020), which may explain their lower homing behaviour compared to females.

Resident behaviour and fidelity may have been underestimated in the present study. First, investigating spawning site fidelity at a greater temporal scale than previous studies implied a more conservative definition of site fidelity. Other studies have focussed their analysis on periods of two to four years (Skjæraasen et al., 2011; de Pontual et al., 2019). We chose to limit the study period to six years to overcome potential changes in the signatures of the water masses and the ontogenetic integration of the elements studied. Second, the behaviour of residents and their site fidelity to very specific spawning areas along the BoB coast may have led to errors in spawning area assignment. For all the seabass tagged at NO, a different spawning area was assigned depending on the data used (DST analysis for the BoB and RF model for the EC). This result tends to indicate a more coastal residency behaviour than their BoB counterparts, as the elemental signature of coastal areas could be similar to that of the EC. Residency behaviour was also observed using acoustic telemetry in the EC area for sub-adults (Stamp et al., 2021).

Why seabass express fidelity and why other do not is an open research question, but evidences from diadromous fish species shows that alternative reproductive strategies (fidelity or straying) is a bet edging strategy improving the overall fitness of species (Hendry et al., 2004). Fidelity can enhance fitness by allowing a fish to reproduce where reproduction has already been successful and straying can enhance fitness by mixing otherwise isolated population, or colonise new spawning areas. Investigating the ability to navigate and to recognize spawning areas requires innovative methods that were not considered in this study, as it implies proximal (imprinting, navigation ability, compass) and distal cues (odours, magnetic field, currents etc.).

4.2 Lack of robust evidence for natal homing

Our results suggest natal homing in seabass but the low number of larval signatures did not provide robust evidence for this behaviour. Natal homing in temperate marine fish species is rarely investigated due to the logistical problems of assigning spawning areas based on natal signatures or tracking individuals from fertilization to spawning on large spatial scales (Bradbury et al., 2008). Nevertheless,

some studies have demonstrated the existence of natal homing on a regional scale for weakfish, a marine fish spawning in estuaries, and on a trans-Atlantic scale for Atlantic Bluefin tuna populations (Thorrold et al., 2001; Rooker et al., 2008). This behaviour deeply structures the populations and high levels of natal homing make the populations more vulnerable to fishing activities (Thorrold et al., 2001). The lack of discrimination of natal signatures between the BoB and the EC was also due to a strong physiological effect on tracer incorporation into otoliths for all the measured trace elements and oxygen isotope ratios. The effects of ontogeny on otolith trace elements have been reported previously in seabass (Reis-Santos et al., 2018) and other temperate fish species (de Pontual et al., 2003; Daverat et al., 2005). Our results confirmed the influence of physiology on the integration of elements in otoliths, with ontogenetic effects being particularly important for physiologically regulated elements such as Mg, Mn and Sr (Thomas and Swearer, 2019; Thomas et al., 2020; Hüssy et al., 2020). Otolith $\delta^{18}O$ was also strongly influenced by ontogenetic changes, with significantly lower ratios in the larval than in the adult stage. Increases in $\delta^{18}O$ concentrations between stages have been reported for other fish species (Shiao et al., 2010; Tanner et al., 2012; Matta et al., 2013) and interpreted as a rapid growth bias in bivalve juveniles (Huyghe et al., 2020). Although these ontogenetic changes are known for most of the elements studied, in this study the large variations in inter individual stage differences could not be corrected. Hence, the RF model fitted on adult data could not be used to assign natal areas and subsequently investigate natal homing.

4.5. Conclusions

We based our study on two types of indirect location information, otolith signatures and DST data, with various spatio-temporal scales of integration. Although DSTs have a higher spatio-temporal resolution than otolith signatures, studying spawning behaviour at the spatial scale of the stock and the temporal scale of the winter (integrating about three months) matches the resolution of the proxies. Seabass is a highly mobile species, capable of migrating over long distances and showing individual histories with high site fidelity to spawning areas. Although we could not prove natal homing, it is suggested in our results. Even if it remains a challenge, further otoliths microchemistry studies would certainly gain

benefit from the analysis of seabass larvae otoliths captured on the spawning sites to obtain references for specific spawning areas. Our results also suggest that seabass stocks are structured, which calls for cautious management in the English Channel, Brittany and the Bay of Biscay as local stock depletion may not be fully compensated by stocks from other spawning areas.

Acknowledgements

We are grateful to the IFREMER colleagues who participated in the tagging surveys and particularly to Stephane Martin who coordinated the recoveries of tagged fish scales and otoliths. Our special thanks go to J. Craven and M. Hall for their help with sample preparation and the SIMS analysis at the NERC, Edinburgh University. We also thank T. Deweulf for his participation in the reading of scales and otoliths to estimate seabass ages.

Competing interests

The authors declare there are no competing interests.

Contributors' statement

ELL: Data curation, Formal analysis, Investigation, Methodology, Resources, Software, Validation, Visualization, Writing - review & editing

FD: Conceptualization, Investigation, Methodology, Resources, Supervision, Roles/Writing - original draft

MW: Formal analysis, Funding acquisition, Methodology, Project administration, Supervision, Writing - review & editing

CP: Methodology, Writing - review & editing

HP: Conceptualization, Funding acquisition, Methodology, Project administration, Resources, Supervision, Writing - review & editing

Funding statement

This study is part of the BARFRAY project funded by the European Maritime and Fisheries Funded (EMFF-OSIRIS N°: PFEA 400017DM0720006)), the French Ministry of Agriculture and Food (MAF), France Filière Pêche (FFP) and IFREMER. The DST data are from the national BarGip project funded by FFP, MAF and IFREMER. The findings and conclusions of the present paper are those of the authors.

Data availability statement

All relevant data are included in the manuscript and its Supporting information files.

References

Anderson, M.J., 2017. Permutational Multivariate Analysis of Variance (PERMANOVA). In Wiley StatsRef: Statistics Reference Online (eds N. Balakrishnan, T. Colton, B. Everitt, W. Piegorsch, F. Ruggeri and J.L. Teugels). https://doi.org/10.1002/9781118445112.stat07841

Artetxe-Arrate, I., Fraile, I., Clear, N., Darnaude, A.M., Dettman, D.L., Pécheyran, C., Farley, J., Murua, H., 2021. Discrimination of yellowfin tuna *Thunnus albacares* between nursery areas in the Indian Ocean using otolith chemistry. Marine Ecology Progress Series 673, 165–181. https://doi.org/10.3354/meps13769

Artetxe-Arrate, I., Fraile, I., Crook, D.A., Zudaire, I., Arrizabalaga, H., Greig, A., Murua, H., 2019. Otolith microchemistry: a useful tool for investigating stock structure of yellowfin tuna (*Thunnus albacares*) in the Indian Ocean. Mar. Freshwater Res. 70, 1708–1721. https://doi.org/10.1071/MF19067

Ayata, S.-D., Lazure, P., Thiébaut, É., 2010. How does the connectivity between populations mediate range limits of marine invertebrates? A case study of larval dispersal between the Bay of Biscay and the English Channel (North-East Atlantic). Progress in Oceanography, 3rd GLOBEC OSM: From ecosystem function to ecosystem prediction 87, 18–36.

Bardarson, H., McAdam, Bruce.J., Thorsteinsson, V., Hjorleifsson, E., Marteinsdottir, G., 2017. Otolith shape differences between ecotypes of Icelandic cod (*Gadus morhua*) with known migratory behaviour inferred from data storage tags. Can. J. Fish. Aquat. Sci. 74, 2122–2130. https://doi.org/10.1139/cjfas-2016-0307

Beraud, C., van der Molen, J., Armstrong, M., Hunter, E., Fonseca, L., Hyder, K., 2018. The influence of oceanographic conditions and larval behaviour on settlement success—the European seabass *Dicentrarchus labrax* (L.). ICES Journal of Marine Science 75, 455–470. https://doi.org/10.1093/icesjms/fsx195

Bradbury, I.R., Campana, S.E., Bentzen, P., 2008. Otolith elemental composition and adult tagging reveal spawning site fidelity and estuarine dependency in rainbow smelt. Marine Ecology Progress Series 368, 255–268. https://doi.org/10.3354/meps07583

Campana, S.E., Thorrold, S.R., 2001. Otoliths, increments, and elements: keys to a comprehensive understanding of fish populations? Can. J. Fish. Aquat. Sci. 58, 30–38. https://doi.org/10.1139/f00-177

Coplen, T.B., Kendall, C., Hopple, J.A., 1983. Comparison of stable isotope reference samples. Nature 302, 236–238.

Cresci, A., Larsen, T., Halvorsen, K. T., Durif, C. M., Bjelland, R., Browman, H. I., Skiftesvik, A. B., 2022. Goldsinny wrasse (*Ctenolabrus rupestris*) have a sex-dependent magnetic compass for maintaining site fidelity. Fisheries Oceanography, 31, 164-171. https://doi.org/10.1111/fog.12569

Dambrine, C., Woillez, M., Huret, M., de Pontual, H., 2021. Characterising Essential Fish Habitat using spatio-temporal analysis of fishery data: A case study of the European seabass spawning areas. Fisheries Oceanography 30, 413–428. https://doi.org/10.1111/fog.12527

Darnaude, A.M., Hunter, E., 2017. Validation of otolith $\delta^{18}O$ values as effective natural tags for shelf-scale geolocation of migrating fish. Marine Ecology Progress Series 598, 167–185. https://doi.org/10.3354/meps12302

Darnaude, A.M., Sturrock, A., Trueman, C.N., Mouillot, D., EIMF, Campana, S.E., Hunter, E., 2014. Listening In on the Past: What Can Otolith $\delta^{18}O$ Values Really Tell Us about the Environmental History of Fishes? PLOS ONE 9, e108539. https://doi.org/10.1371/journal.pone.0114951

Daverat, F., Tomas, J., Lahaye, M., Palmer, M., Elie, P., 2005. Tracking continental habitat shifts of eels using otolith Sr/Ca ratios: validation and application to the coastal, estuarine and riverine eels of the Gironde–Garonne–Dordogne watershed. Mar. Freshwater Res. 56, 619–627. https://doi.org/10.1071/MF04175

de Pontual, H., Lagardère, F., Amara, R., Bohn, M., Ogor, A., 2003. Influence of ontogenetic and environmental changes in the otolith microchemistry of juvenile sole (*Solea solea*). Journal of Sea Research, Proceedings of the Fifth International Symposium on Flatfish Ecology, Part I 50, 199–211. https://doi.org/10.1016/S1385-1101(03)00080-7

de Pontual, H., Lalire, M., Fablet, R., Laspougeas, C., Garren, F., Martin, S., Drogou, M., Woillez, M., 2019. New insights into behavioural ecology of European seabass off the West Coast of France: implications at local and population scales. ICES J Mar Sci 76, 501–515. https://doi.org/10.1093/icesjms/fsy086

de Pontual, H., Heerah, K., Goossens, J., Garren, F., Martin, S., Le Ru, L., Le Roy, D., Woillez, M. Seasonal migration, site fidelity and population structure of European seabass: shedding light from large-scale electronic tagging. Manuscript submitted for publication.

de Villiers, S., 1999. Seawater strontium and Sr/Ca variability in the Atlantic and Pacific oceans. Earth and Planetary Science Letters, 171, 623-634. https://doi.org/10.1016/S0012-821X(99)00174-0

Elsdon, T., Wells, B., Campana, S., Gillanders, B., Jones, C., Limburg, K., Secor, D., Thorrold, S., Walther, B., 2008. Otolith Chemistry To Describe Movements And Life-History Parameters Of Fishes, in: Oceanography and Marine Biology - An Annual Review. pp. 297–330. https://doi.org/10.1201/9781420065756.ch7

Elsdon, T.S., Gillanders, B.M., 2005. Alternative life-history patterns of estuarine fish: barium in otoliths elucidates freshwater residency. Can. J. Fish. Aquat. Sci. 62, 1143–1152. https://doi.org/10.1139/f05-029

Fritsch, M., Morizur, Y., Lambert, E., Bonhomme, F., Guinand, B., 2007. Assessment of seabass (*Dicentrarchus labrax*, L.) stock delimitation in the Bay of Biscay and the English Channel based on mark-recapture and genetic data. Fisheries Research 83, 123–132. https://doi.org/10.1016/j.fishres.2006.09.002

Fromentin, J.-M., Ernande, B., Fablet, R., de Pontual, H., 2009. Importance and future of individual markers for the ecosystem approach to fisheries. Aquatic Living Resources 22, 395–408. https://doi.org/10.1051/alr/2009035

Gatti, P., Fisher, J.A.D., Cyr, F., Galbraith, P.S., Robert, D., Le Bris, A., 2021. A review and tests of validation and sensitivity of geolocation models for marine fish tracking. Fish and Fisheries 22, 1041–1066. https://doi.org/10.1111/faf.12568

Harwood, A.J.P., Dennis, P.F., Marca, A.D., Pilling, G.M., Millner, R.S., 2008. The oxygen isotope composition of water masses within the North Sea. Estuarine, Coastal and Shelf Science 78, 353–359. https://doi.org/10.1016/j.ecss.2007.12.010

Heimbrand, Y., Limburg, K.E., Hüssy, K., Casini, M., Sjöberg, R., Palmén Bratt, A.-M., Levinsky, S.-E., Karpushevskaia, A., Radtke, K., Öhlund, J., 2020. Seeking the true time: Exploring otolith chemistry as an age-determination tool. Journal of Fish Biology 97, 552–565. https://doi.org/10.1111/jfb.14422

Hendry, A. P., Castric, V., Kinnison, M. T., Quinn, T. P., Hendry, A., Stearns, S., 2004. The evolution of philopatry and dispersal. *Evolution illuminated: salmon and their relatives*, p.52-91.

Horne, C. R., Hirst, A. G., Atkinson, D., 2020. Selection for increased male size predicts variation in sexual size dimorphism among fish species. Proceedings of the Royal Society B. 287:20192640.20192640. https://doi.org/10.1098/rspb.2019.2640

Hüssy, K., Limburg, K.E., de Pontual, H., Thomas, O.R.B., Cook, P.K., Heimbrand, Y., Blass, M., Sturrock, A.M., 2020. Trace Element Patterns in Otoliths: The Role of Biomineralization. Reviews in Fisheries Science & Aquaculture 0, 1–33. https://doi.org/10.1080/23308249.2020.1760204

Hüssy, K., Nielsen, B., Mosegaard, H., Worsøe Clausen, L., 2009. Using data storage tags to link otolith macrostructure in Baltic cod *Gadus morhua* with environmental conditions. Marine Ecology - Progress Series 378, 161–170. https://doi.org/10.3354/meps07876

Huyghe, D., Emmanuel, L., de Rafelis, M., Renard, M., Ropert, M., Labourdette, N., Lartaud, F., 2020. Oxygen isotope disequilibrium in the juvenile portion of oyster shells biases seawater temperature reconstructions. Estuarine, Coastal and Shelf Science 240, 106777. https://doi.org/10.1016/j.ecss.2020.106777

ICES, 2020a. Seabass (*Dicentrarchus labrax*) in divisions 8.a–b (northern and central Bay of Biscay). In Report of the ICES Advisory Committee, 2020. ICES Advice 2020, bss.27.8ab.

ICES, 2020b. Seabass (*Dicentrarchus labrax*) in divisions 4.b–c, 7.a, and 7.d–h (central and southern North Sea, Irish Sea, English Channel, Bristol Channel, and Celtic Sea. In Report of the ICES Advisory Committee, 2020. ICES Advice 2020, bss.27.4bc7ad-h.

Jennings, S., Pawson, M.G., 1992. The origin and recruitment of bass, *Dicentrarchus labrax*, larvae to nursery areas. Journal of the Marine Biological Association of the United Kingdom 72, 199–212. https://doi.org/10.1017/S0025315400048888

Jónsson, E.P., Campana, S.E., Sólmundsson, J., Jakobsdóttir, K.B., Bárðarson, H., 2021. Otolith-based discrimination of cod ecotypes and the effect of growth rate. https://doi.org/10.1101/2021.02.11.430748

Kerr, L.A., Hintzen, N.T., Cadrin, S.X., Clausen, L.W., Dickey-Collas, M., Goethel, D.R., Hatfield, E.M.C., Kritzer, J.P., Nash, R.D.M., 2017. Lessons learned from practical approaches to reconcile mismatches between biological population structure and stock units of marine fish. ICES Journal of Marine Science 74, 1708–1722. https://doi.org/10.1093/icesjms/fsw188

Kim, S.-T., O'Neil, J., Hillaire-Marcel, C., Mucci, A., 2007. Oxygen isotope fractionation between synthetic aragonite and water: Influence of temperature and Mg2+ concentration. Geochimica et Cosmochimica Acta 71, 4704–4715. https://doi.org/10.1016/j.gca.2007.04.019

LeGrande, A.N., Schmidt, G.A., 2006. Global gridded data set of the oxygen isotopic composition in seawater. Geophysical Research Letters 33. https://doi.org/10.1029/2006GL026011

Matta, M.E., Orland, I.J., Ushikubo, T., Helser, T.E., Black, B.A., Valley, J.W., 2013. Otolith oxygen isotopes measured by high-precision secondary ion mass spectrometry reflect life history of a yellowfin sole (*Limanda aspera*). Rapid Communications in Mass Spectrometry 27, 691–699. https://doi.org/10.1002/rcm.6502

Mercier, L., Darnaude, A.M., Bruguier, O., Vasconcelos, R.P., Cabral, H.N., Costa, M.J., Lara, M., Jones, D.L., Mouillot, D., 2011. Selecting statistical models and variable combinations for optimal classification using otolith microchemistry. Ecol Appl 21, 1352–1364. https://doi.org/10.1890/09-1887.1

Miralles, L., Juanes, F., Garcia-Vazquez, E., 2014. Interoceanic Sex-Biased Migration in Bluefish, Transactions of the American Fisheries Society, 143:5, 1308-1315. https://doi.org/10.1080/00028487.2014.935480

Muths, D., Grewe, P., Jean, C., Bourjea, J., 2009. Genetic population structure of the Swordfish (*Xiphias gladius*) in the southwest Indian Ocean: Sex-biased differentiation, congruency between markers and its incidence in a way of stock assessment. Fisheries Research, 97, 263-269. https://doi.org/10.1016/j.fishres.2009.03.004

Neves, A., Vieira, A.R., Sequeira, V., Paiva, R.B., Janeiro, A.I., Gaspar, L.M., Gordo, L.S., 2019. Otolith shape and isotopic ratio analyses as a tool to study *Spondyliosoma cantharus* population structure. Marine Environmental Research 143, 93–100. https://doi.org/10.1016/j.marenvres.2018.11.012

Pawson, M.G., Pickett, G.D., Leballeur, J., Brown, M., Fritsch, M., 2007. Migrations, fishery interactions, and management units of seabass (*Dicentrarchus labrax*) in Northwest Europe. ICES J Mar Sci 64, 332–345. https://doi.org/10.1093/icesjms/fsl035

Petitgas, P., Rijnsdorp, A.D., Dickey-Collas, M., Engelhard, G.H., Peck, M.A., Pinnegar, J.K., Drinkwater, K., Huret, M., Nash, R.D.M., 2013. Impacts of climate change on the complex life cycles of fish. Fisheries Oceanography 22, 121–139. https://doi.org/10.1111/fog.12010

Pickett, G.D., Pawson, M.G., 1994. Seabass: Biology, exploitation and conservation. Chapman & Hall. London and Glasgow. 342p

Pickett, G.D., Kelley, D.F., Pawson, M.G., 2004. The patterns of recruitment of sea bass, *Dicentrarchus labrax* L. from nursery areas in England and Wales and implications for fisheries management. Fisheries Research 68, 329–342. https://doi.org/10.1016/j.fishres.2003.11.013

Pinto, M., Monteiro, J.N., Crespo, D., Costa, F., Rosa, J., Primo, A.L., Pardal, M.A., Martinho, F., 2021. Influence of oceanic and climate conditions on the early life history of European seabass *Dicentrarchus labrax*. Marine Environmental Research 169, 105362. https://doi.org/10.1016/j.marenvres.2021.105362

Reis-Santos, P., Tanner, S.E., Elsdon, T.S., Cabral, H.N., Gillanders, B.M., 2013. Effects of temperature, salinity and water composition on otolith elemental incorporation of *Dicentrarchus labrax*. Journal of Experimental Marine Biology and Ecology 446, 245–252. https://doi.org/10.1016/j.jembe.2013.05.027

Reis-Santos, P., Vasconcelos, R.P., Tanner, S.E., Fonseca, V.F., Cabral, H.N., Gillanders, B.M., 2018. Extrinsic and intrinsic factors shape the ability of using otolith chemistry to characterize estuarine environmental histories. Marine Environmental Research 140, 332–341. https://doi.org/10.1016/j.marenvres.2018.06.002

Rideout, R. M., Tomkiewicz, J., 2011. Skipped Spawning in Fishes: More Common than You Might Think, Marine and Coastal Fisheries, 3:1, 176-189. https://doi.org/10.1080/19425120.2011.556943

Robinet, T., Roussel, V., Cheze, K., Gagnaire, P.-A., 2020. Spatial gradients of introgressed ancestry reveal cryptic connectivity patterns in a high gene flow marine fish. Molecular Ecology 29, 3857–3871. https://doi.org/10.1111/mec.15611

Rooker, J., Secor, D., DeMetrio, G., Kaufman, A., Belmonte Rios, A., Tičina, V., 2008. Evidence of trans-Atlantic movement and natal homing of bluefin tuna from stable isotopes in otoliths. Marine Ecology-progress Series - MAR ECOL-PROGR SER 368, 231–239. https://doi.org/10.3354/meps07602

Saillant, E., Fostier, A., Menu, B., Haffray, P., Chatain, B., 2001. Sexual growth dimorphism in sea bass *Dicentrarchus labrax*. Aquaculture 202, 371–387. https://doi.org/10.1016/S0044-8486(01)00786-4

Shiao, J.-C., Wang, S.-W., Yokawa, K., Ichinokawa, M., Takeuchi, Y., Chen, Y.-G., Shen, C.-C., 2010. Natal origin of Pacific bluefin tuna *Thunnus orientalis* inferred from otolith oxygen isotope composition. Marine Ecology Progress Series 420, 207–219. https://doi.org/10.3354/meps08867

Skjæraasen, J.E., Meager, J.J., Karlsen, Ø., Hutchings, J.A., Fernö, A., 2011. Extreme spawning-site fidelity in Atlantic cod. ICES Journal of Marine Science 68, 1472–1477. https://doi.org/10.1093/icesjms/fsr055

Soeth, M., Spach, H.L., Daros, F.A., Adelir-Alves, J., de Almeida, A.C.O., Correia, A.T., 2019. Stock structure of Atlantic spadefish *Chaetodipterus faber* from Southwest Atlantic Ocean inferred from otolith elemental and shape signatures. Fisheries Research 211, 81–90. https://doi.org/10.1016/j.fishres.2018.11.003

Souche, E.L., Hellemans, B., Babbucci, M., MacAoidh, E., Guinand, B., Bargelloni, L., Chistiakov, D.A., Patarnello, T., Bonhomme, F., Martinsohn, J.T., Volckaert, F.A.M., 2015. Range-wide population structure of European seabass *Dicentrarchus labrax*. Biological Journal of the Linnean Society 116, 86–105. https://doi.org/10.1111/bij.12572

Stamp, T., Clarke, D., Plenty, S., Robbins, T., Stewart, J.E., West, E., Sheehan, E., 2021. Identifying juvenile and sub-adult movements to inform recovery strategies for a high value fishery - European bass (*Dicentrarchus labrax*). ICES Journal of Marine Science 78, 3121–3134. https://doi.org/10.1093/icesjms/fsab180

Tanner, S.E., Reis-Santos, P., Cabral, H.N., 2016. Otolith chemistry in stock delineation: A brief overview, current challenges and future prospects. Fisheries Research, Advances in Fish Stock Delineation 173, 206–213. https://doi.org/10.1016/j.fishres.2015.07.019

Tanner, S.E., Vasconcelos, R.P., Cabral, H.N., Thorrold, S.R., 2012. Testing an otolith geochemistry approach to determine population structure and movements of European hake in the northeast Atlantic Ocean and Mediterranean Sea. Fisheries Research 125–126, 198–205. https://doi.org/10.1016/j.fishres.2012.02.013

Thomas, O.R.B., Richards, K.L., Petrou, S., Roberts, B.R., Swearer, S.E., 2020. In situ 3D visualization of biomineralization matrix proteins. Journal of Structural Biology 209, 107448. https://doi.org/10.1016/j.jsb.2020.107448

Thomas, O.R.B., Swearer, S.E., 2019. Otolith Biochemistry—A Review. Reviews in Fisheries Science & Aquaculture 27, 458–489. https://doi.org/10.1080/23308249.2019.1627285

673 Thorrold, S.R., Latkoczy, C., Swart, P.K., Jones, C.M., 2001. Natal homing in a marine fish metapopulation.
674 Science 291, 297–299. https://doi.org/10.1126/science.291.5502.297

675 Trueman, C.N., MacKenzie, K.M., Palmer, M.R., 2012. Identifying migrations in marine fishes through
676 stable-isotope analysis. Journal of Fish Biology 81, 826–847. https://doi.org/10.1111/j.1095-
677 8649.2012.03361.x

678 von Leesen, G., Bjarte Bogstad, B., Einar Hjörleifsson, E., Ulysses S. Ninnemann, U. S., Campana, S., E.
679 2021. Temperature exposure in cod driven by changes in abundance. Canadian Journal of Fisheries and
680 Aquatic Sciences. 79(4): 587-600. https://doi.org/10.1139/cjfas-2020-0424

681 Woillez, M., Fablet, R., Ngo, T.T., Lalire, M., Lazure, P., Garren, F., de Pontual, H., 2016. A HMM-based
682 model to geolocate pelagic fish from high-resolution individual temperature and depth histories:
683 European seabass as a case study. Ecological Modelling 321.
684 https://doi.org/10.1016/j.ecolmodel.2015.10.024

685 Wolgemuth, K., Broecker, W.S., 1970. Barium in sea water. Earth and Planetary Science Letters 8, 372–
686 378. https://doi.org/10.1016/0012-821X(70)90110-X

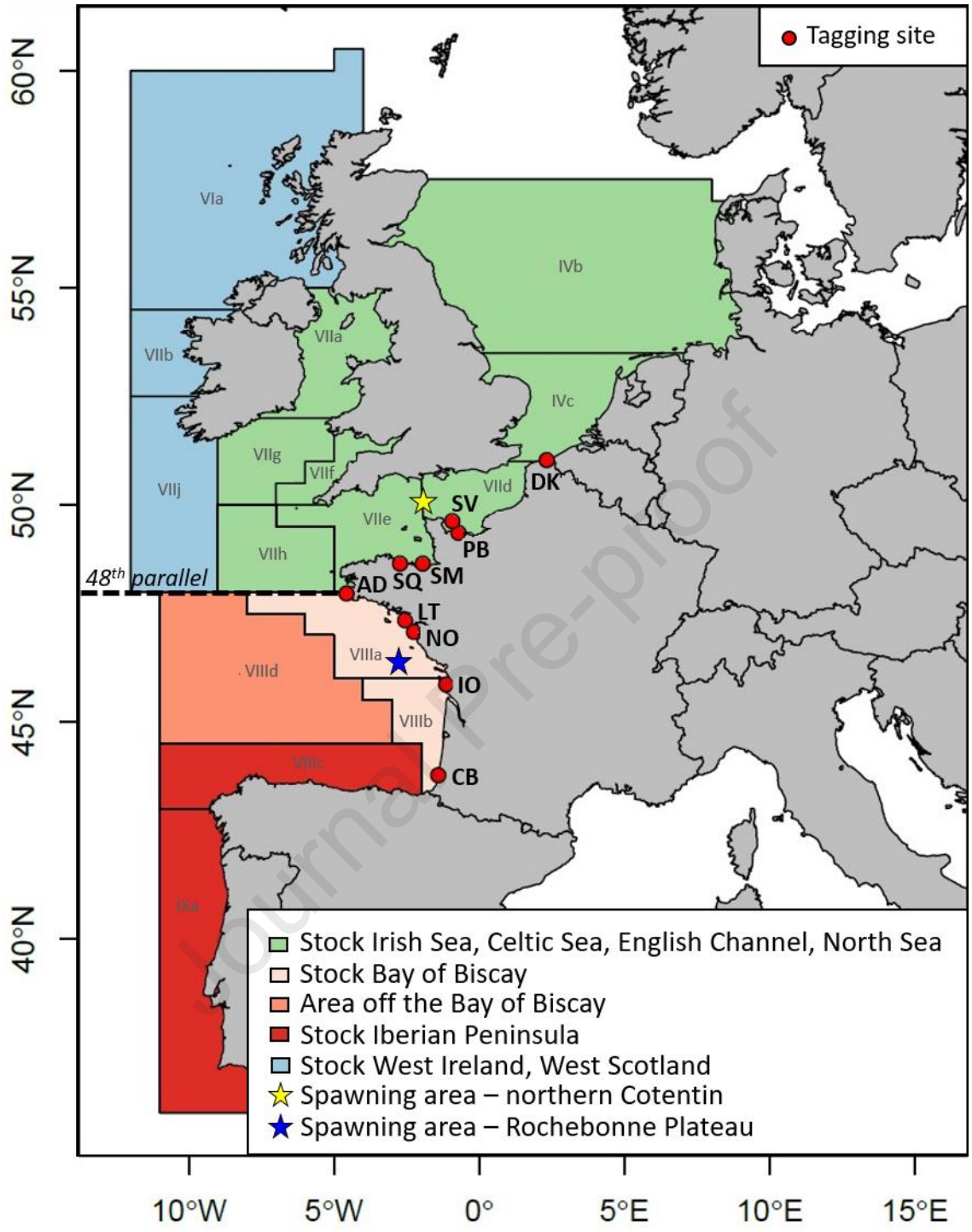

Figure.1. Location of the four seabass stocks considered by ICES in the northeast Atlantic and tagging sites in this study (red points). Adapted from de Pontual et al. (submitted); full site names are available in Supp. Mat. 1.

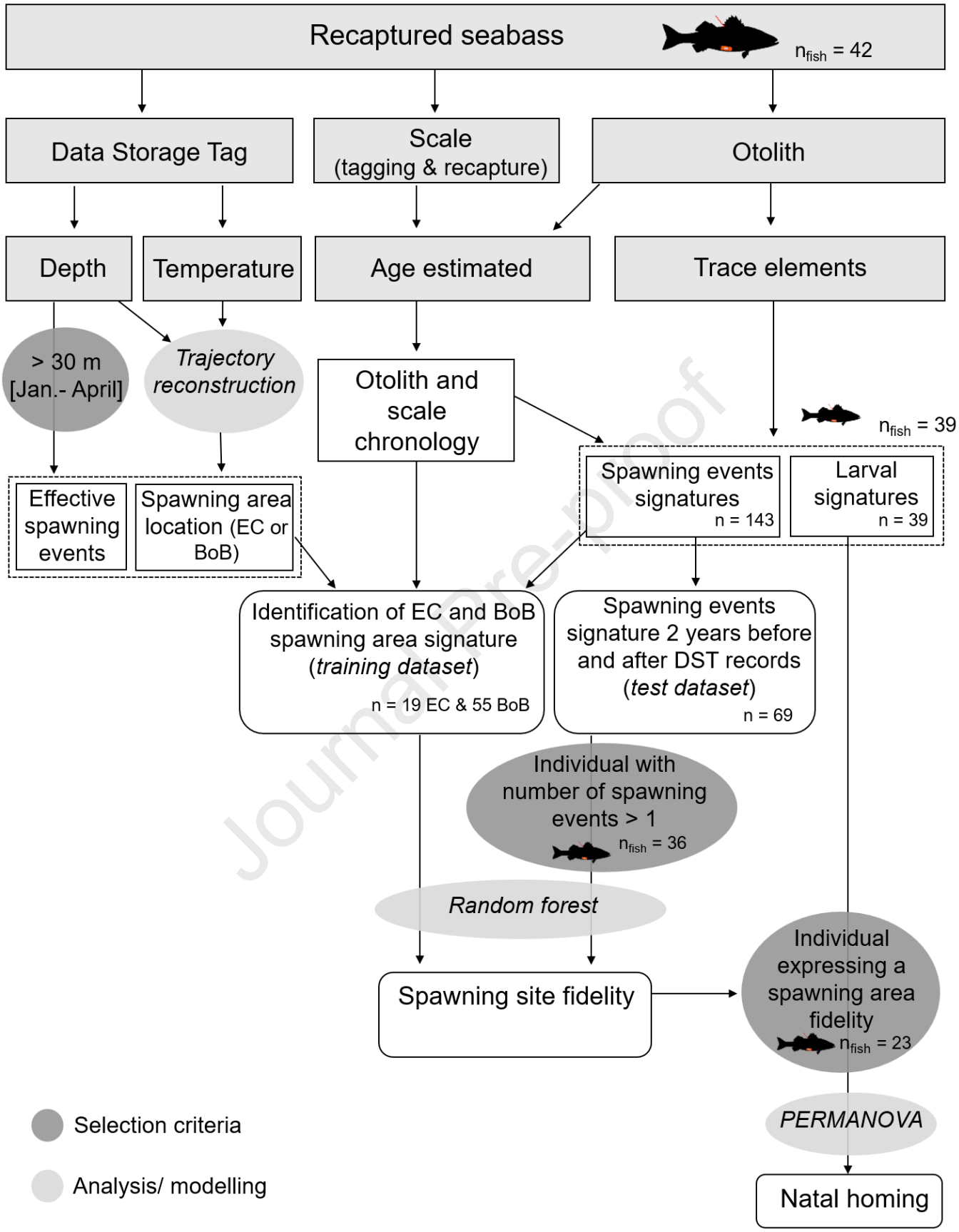

Figure. 2. Work flow diagram of the methodology used to explore seabass spawning area fidelity and natal homing.

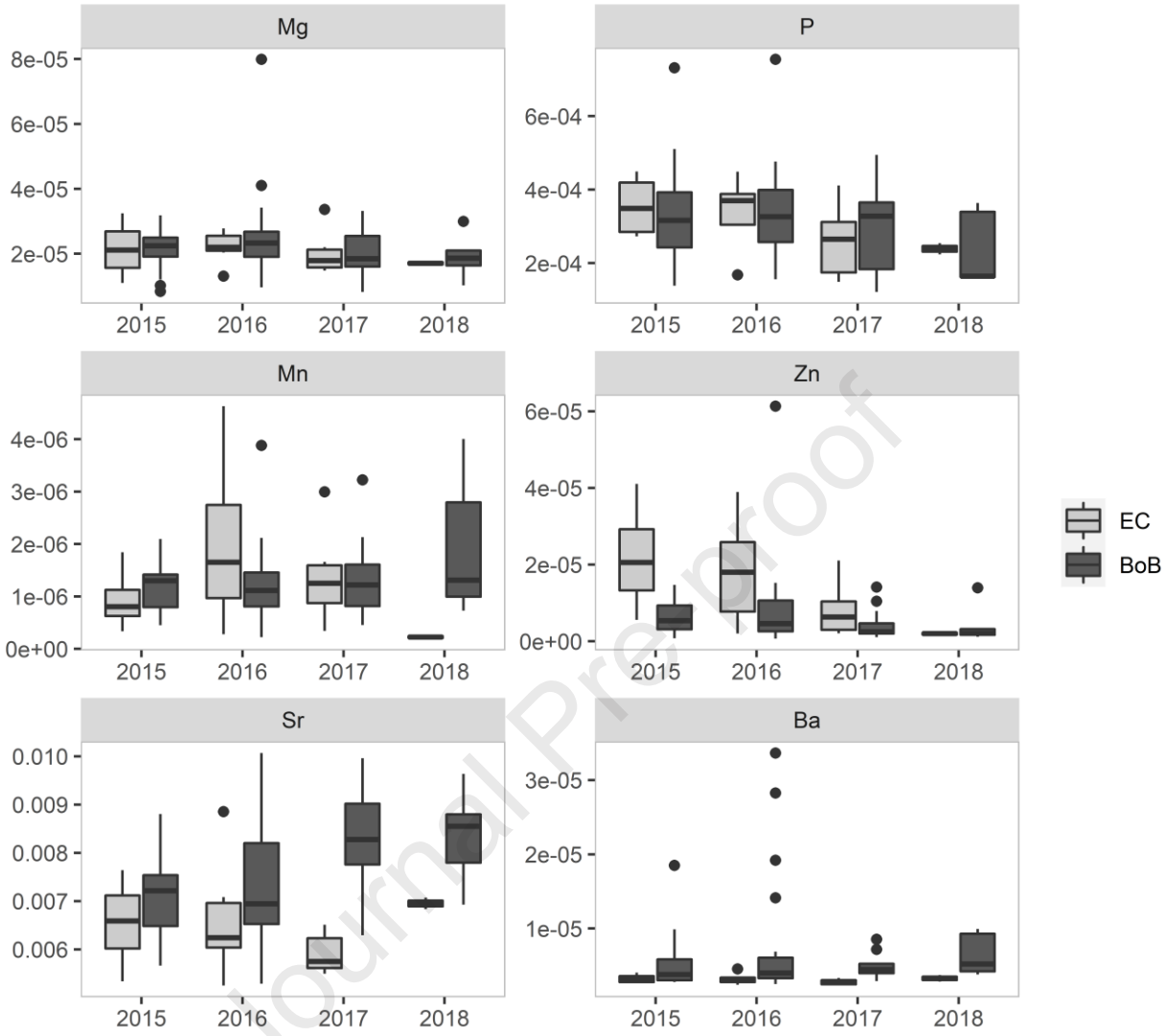

Figure. 3. Boxplots of elemental concentrations w.r.t. years. The training dataset consists of adult otoliths (for which otolith winter signatures were coupled to DST assigned spawning area).

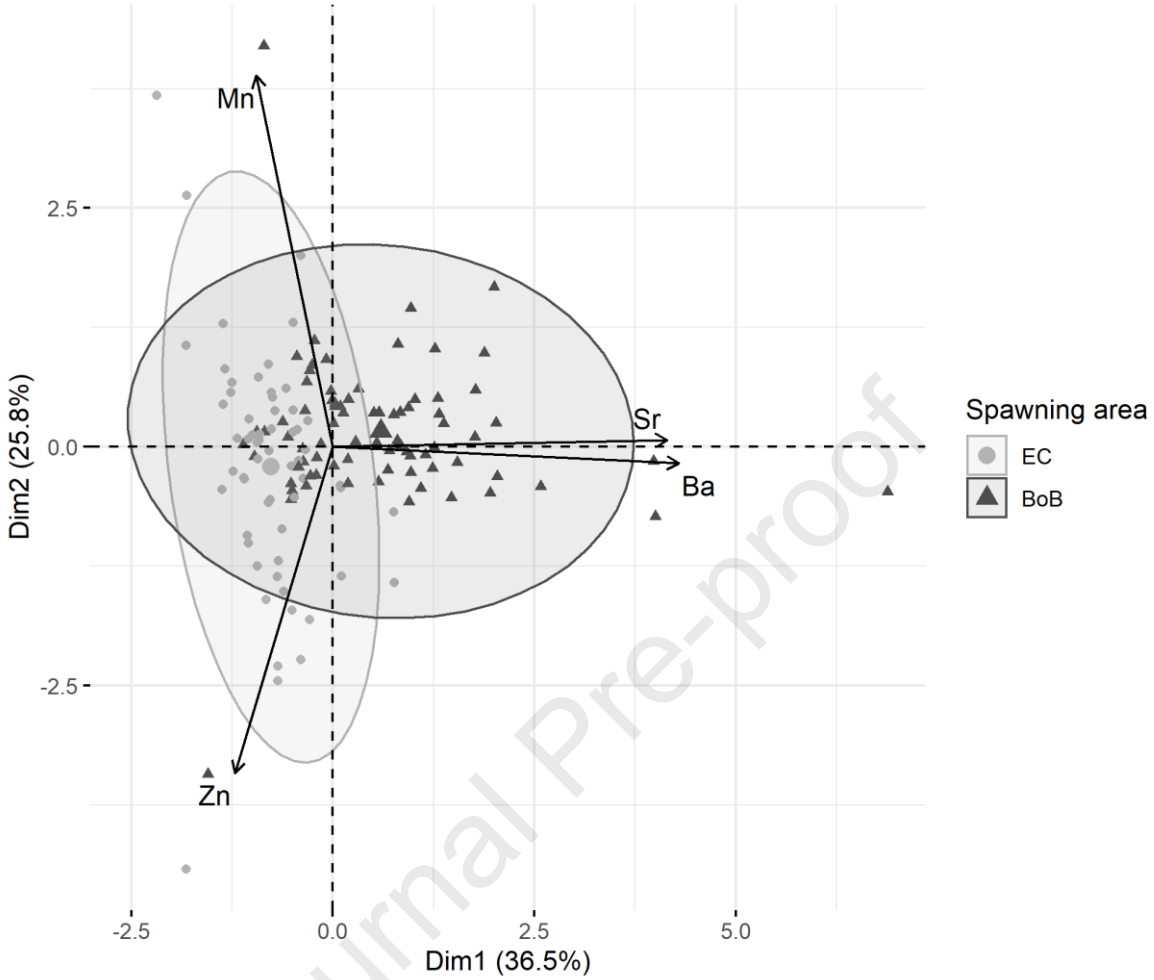

Figure. 4. Principal Component Analysis of winter spawning signatures based on seabass that expressed fidelity to a spawning area (EC or BoB).

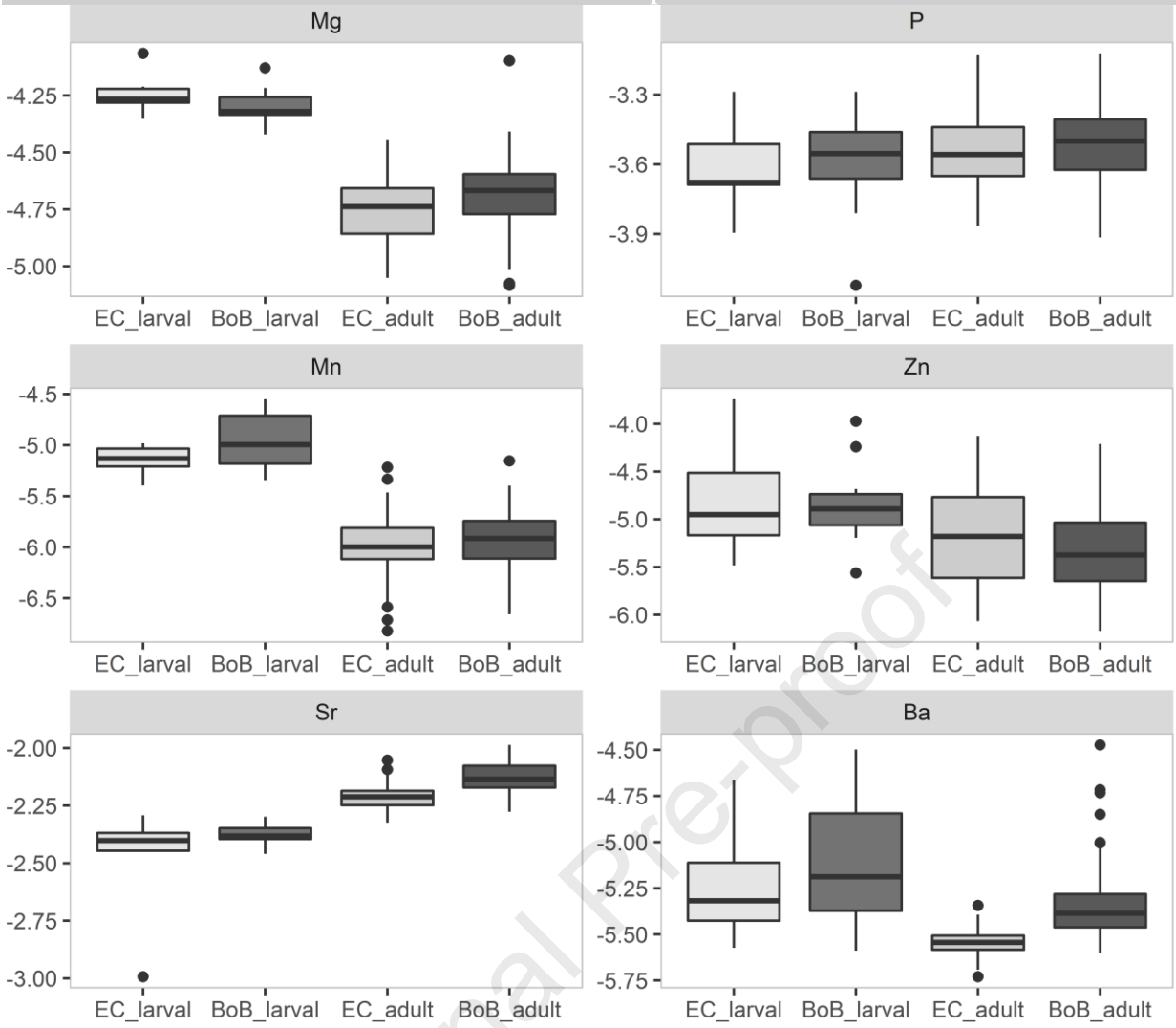

Figure. 5. Boxplots of larval and adult trace elements signatures (log-transformed) for the 23 seabass that expressed fidelity to a spawning area. (EC: English Channel, BoB: Bay of Biscay)

Table 1. Results of the PERMANOVA testing the effects of spawning areas, years and the interaction between years and spawning areas on the trace elements for the training dataset (coupled DST/otolith composition). Significant effects are indicated in bold.

Element	Factor	SS	R^2	F	p
Mg	Spawning area	3.48e-11	0.005	0.363	0.550
	Year	4.37e-11	0.006	0.456	0.500
	Spawning area:Year	5.10e-12	0.0007	0.053	0.804
P	Spawning area	1.78e-09	0.001	0.120	0.744
	Year	6.48e-08	0.058	4.388	**0.039**
	Spawning area:Year	4.30e-09	0.003	0.290	0.597
Mn	Spawning area	6.10e-14	0.001	0.075	0.801
	Year	5.37e-13	0.009	0.661	0.407
	Spawning area:Year	1.65e-12	0.027	2.035	0.158
Zn	Spawning area	7.93e-10	0.103	9.178	**0.005**
	Year	3.93e-10	0.051	4.554	**0.025**
	Spawning area:Year	4.62e-10	0.060	5.346	**0.026**
Sr	Spawning area	1.84e-05	0.171	16.654	**0.001**
	Year	7.48e-06	0.069	6.770	**0.008**
	Spawning area:Year	4.00e-06	0.037	3.622	0.073
Ba	Spawning area	1.47e-10	0.070	5.349	**0.020**
	Year	2.00e-13	0.0001	0.007	0.934
	Spawning area:Year	3.00e-14	0.00002	0.001	0.973

Highlights

- Investigation of seabass spawning site fidelity and natal homing.
- Data Storage Tag information was coupled to otolith microchemistry to infer spawning areas.
- Spawning site fidelity was found for most seabass individuals (64 %).
- Otolith tracers (elements and $\delta^{18}O$) were significantly biased by ontogenetic effects.
- Homing behaviour results were inconclusive.

Declaration of interests

☒ The authors declare that they have no known competing financial interests or personal relationships that could have appeared to influence the work reported in this paper.

☐ The authors declare the following financial interests/personal relationships which may be considered as potential competing interests: